Childs Nerv Syst (2018) 34:267–276
DOI 10.1007/s00381-017-3565-0

ORIGINAL PAPER

Next generation of ventricular catheters for hydrocephalus based on parametric designs

M. Galarza[1] · A. Giménez[2] · J. M. Amigó[2] · M. Schuhmann[3] · R. Gazzeri[4] · U. Thomale[5] · J. P. McAllister 2nd[6]

Received: 12 June 2017 / Accepted: 2 August 2017 / Published online: 15 August 2017

Abstract

Background The flow pattern of the cerebrospinal fluid is probably the most important factor related to obstruction of ventricular catheters during the normal treatment of hydrocephalus. To better comprehend the flow pattern, we have carried out a parametric study via numerical models of ventricular catheters. In previous studies, the flow was studied under steady and, recently, in pulsatile boundary conditions by means of computational fluid dynamics (CFD) in three-dimensional catheter models.

Objective This study aimed to bring in prototype models of catheter CFD flow solutions as well to introduce the theory behind parametric development of ventricular catheters.

Methods A preceding study allowed deriving basic principles which lead to designs with improved flow patterns of ventricular catheters. The parameters chosen were the number of drainage segments, the distances between them, the number and diameter of the holes on each segment, as well as their relative angular position.

Results CFD results of previously unreleased models of ventricular catheter flow solutions are presented in this study. Parametric development guided new designs with better flow distribution while lowering the shear stress of the catheters holes. High-resolution 3D printed catheter solutions of three models and basic benchmark testing are introduced as well.

Conclusions The next generation of catheter with homogeneous flow patterns based on parametric designs may represent a step forward for the treatment of hydrocephalus, by possibly broadening their lifespan.

Keywords Catheter obstruction · Shunt revision · Flow · Cerebrospinal fluid · Cerebral ventricle · Catheter prototypes

Introduction

Hydrocephalus is a complex cerebral disease basically consisting of an abnormal accumulation of cerebrospinal fluid (CSF) in the ventricular cavities of the brain. All of the ventricular cavities are interconnected, thus allowing the CSF to circulate. Hydrocephalus is usually caused by a disturbance in the production, circulation, or absorption of CSF, with ventricular enlargement being one of the leading characteristics of this condition (1–4). Most commonly, to treat hydrocephalus, a silicone catheter is inserted in one of the ventricles which is then connected to a regulation valve, to drain the excess of CSF and divert it to another body cavity. Although a typical shunt system is composed with three parts, i.e., ventricular catheter, valve, and distal catheter, the typical shunt malfunction occurs at the ventricular catheter mainly in the pediatric population; while most studies regarding shunt systems were proposed at valve devices. Moreover, there is no reason

✉ M. Galarza
m.galarza@um.es

1 Regional Service of Neurosurgery, University of Murcia, Murcia, Spain

2 Operations Research Center, University Miguel Hernández de Elche, Alacant, Spain

3 Department of Neurosurgery, University Hospital Tuebingen, Eberhard-Karls-University, Tuebingen, Germany

4 Department of Neurosurgery, San Giovanni Addolorata Hospital, Rome, Italy

5 Charité Universitätsmedizin Berlin, Campus Virchow, Klinikum, Augustenburger Platz 1, Berlin, Germany

6 Department of Neurological Surgery, Washington University School of Medicine, St. Louis, MI, USA

beyond technical simplicity, why most ventricular catheter manufacturers produce only typical standard designs. In addition, there are myriads of patented models of ventricular catheters; some of them seems not expected to achieve the intended purpose from a clinical and practical point of view, while others are useless from a hydrodynamic point of view.

A ventricular catheter, which can be inserted from the frontal and occipital/parietal burr hole, has usually three inlet drainage parts, depending on the ventricular anatomy, the longitude of the catheter within the ventricle, and the longitude of the inlet segment within the ventricle (Fig. 1). For specifications, please refer to (5). These factors determine how the catheter interacts with the ventricle walls, the choroid plexus and, depending on the CSF characteristics (clear, purulent, hemorrhagic, etc.), the cells and proteins (Fig. 2). Evidently, this interaction determines in part the obstruction of the ventricular catheter which is, overall, the most common complication during treatment of hydrocephalus (Fig. 3). The other key factor is flow.

In (6), we analyzed the fluid dynamics of five currently in use ventricular catheters to evaluate flow factors of proximal shunt malfunction. We found that the flow distribution follows a similar pattern in all ventricular catheters considered. In fact, from 50 to 75% of the cerebrospinal fluid flows into proximal sets of inlets of current commercially available 12- to 32-hole ventricular catheters, the flow being most uniform for the model Rivulet (7). We concluded that occlusion is most likely to occur at the proximal inlets in ventricular catheters, i.e., holes located on the segment closest to the valve or furthest from the tip of the ventricular catheter. These results concur

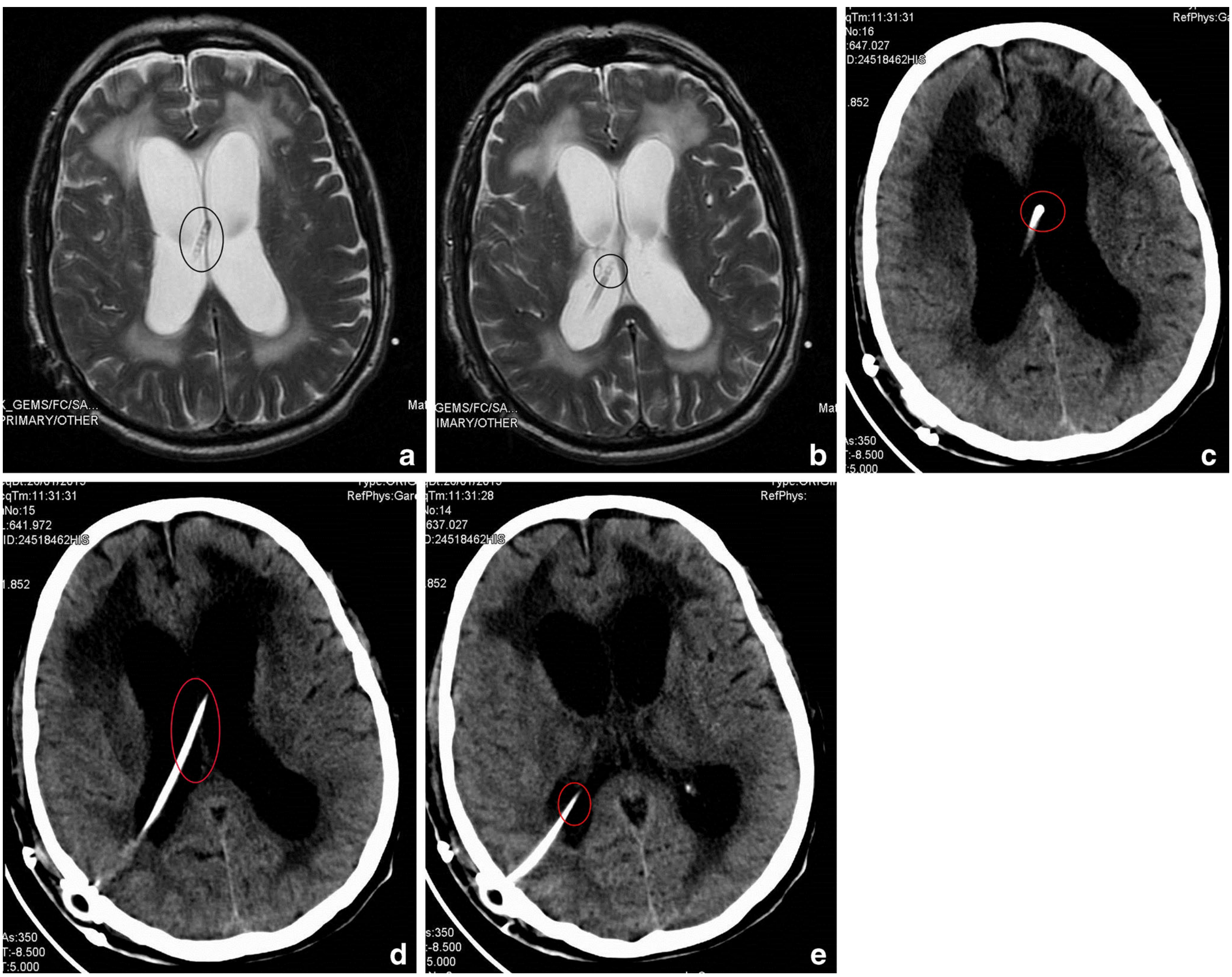

Fig. 1 MR T2-weighted images of hydrocephalus treated with a shunt. Ventricular catheter with evident open inlets in the lateral ventricle of the brain shows its most distal part in contact with the septum pellucidum (**a**) while the most proximal are directly in contact with the choroid plexus (**b**). CAT scan images showing hydrocephalus with a shunt and a ventricular catheter inserted in the occipital horn of the cerebrum. In this case, we deduce that there are *three different parts of the catheter*: a distal part in contact with the septum pellucidum (**c**), a medial part within the ventricle (**d**), and a proximal part in contact with the choroid plexus and brain (**e**). The perforated or inlet part of the catheter within the ventricle is not excluding an occlusion of the VC

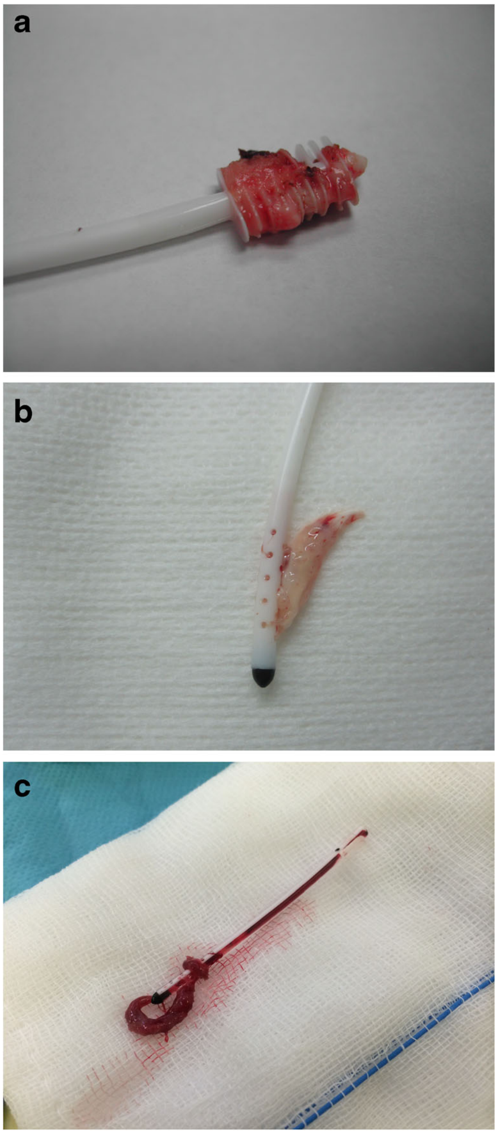

Fig. 2 A series of removed ventricular catheters with total occlusion due to brain tissue and choroid plexus. The first photograph depicts a Portnoy catheter with brain embedded in its flanges (**a**). Other cases mainly disclosed brain tissue obstructing the perforated or inlet part of the catheter (**b**). A removed ventricular catheter with total occlusion showing remnants of hemorrhage (**c**). The depicted cases show removed catheters with blood remnants. This occurrence happens due to brain tissue and choroid plexus tearing during removal. Consequences in these cases can be catastrophic; not saying lethal

with the first-time study application of 2-D CFD to ventricular catheters by Lin et al. in 2003 (8).

It is well known that the most frequent cause of shunt failure is ventricular catheter obstruction, which may account for 50 to 80% of newly inserted shunts in children (8, 9). Although many factors contribute to this (8–11), the main one is related to fluid flow characteristics of the ventricular catheter within the hydrocephalic brain (5, 12–17). Numerical simulation is extensively applied in everyday engineering studies to solve efficiently a wide variety of physical and technical problems. In particular, CFD is a numerical method to calculate the flow of compressible and incompressible fluids even with complex geometries, thus providing a functional tool for design optimization (18, 19). Given a 3D model of the system to be studied, and the initial and boundary conditions, the CFD software calculates the resulting flow with greater spatial and temporal resolution than that achieved with specific MRI studies while also displaying other flow characteristics like pressures, flow structures, stresses, and pressure waves (5, 6, 13, 18, 19).

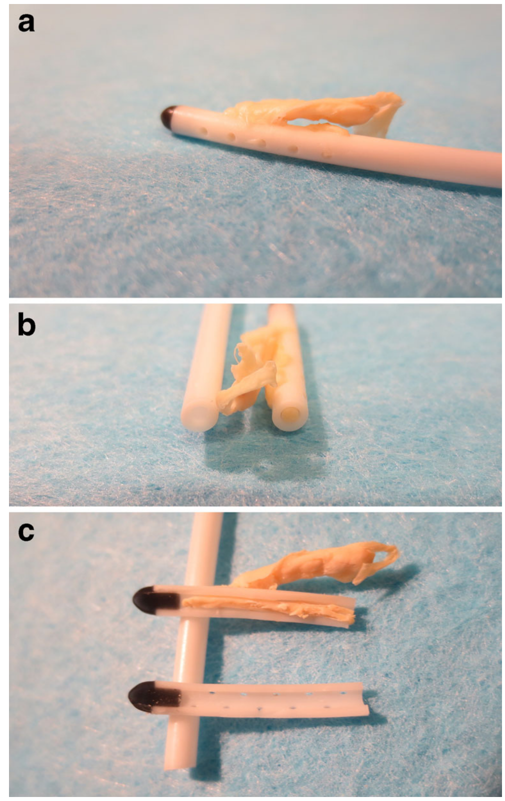

Fig. 3 A case of a totally occluded ventricular catheter due to brain tissue. We cut it at the most proximal hole and disclosed a complete occlusion at that level with a persisting patent rest of the catheter. Thereafter, we did split the occluded catheter in half lengthwise to verify visually where exactly luminal blockage occurred. **a** A totally occluded ventricular catheter due to brain tissue. **b** Complete occlusion at the most proximal hole in the ventricular catheter. **c** Brain tissue infiltrated the holes only on one side. In this case, the brain tissue infiltrated the holes completely on one side, while the other side was quite free

Previously, an extensive parametric study disclosed the attaining of basic principles leading to improvement of the flow pattern in all ventricular catheters (14). In the present study, we introduce ventricular catheter models based on parametric data. The catheters proposed herein achieve the same goal as the Rivulet catheter, namely, to homogenize the distribution of the flows through the drainage rings but without necessarily varying the diameters of the holes.

Methods

The physical problem we conceived in this study is the flow of a simple, incompressible fluid that is the cerebrospinal fluid, through a ventricular catheter placed inside a cavity. The fluid flows into the cavity through an inlet and exit through the lumen of the ventricular catheter. Designs were all prototype models in this study. To deal with this problem, we build a numerical model of the physical domain, i.e., ventricular catheter and cavity, and solve the Navier-Stokes equations numerically with appropriate initial and boundary conditions. Our analysis tool is computational fluid dynamics developed in three dimensions.

A numerical model consists of three basic steps: data pre-processing, solving process, and data post-processing. In the pre-processing step, the computational domain and the meshing of the model are built, and the initial and boundary conditions are fixed. Next, a suitable numerical scheme is implemented to solve the governing equations of the model. Lastly, in the processing step, a correct analysis and visualization of the data are required to ensure a proper discussion of the results. It is therefore customary in CFD to use numerous software tools to carry out a numerical experiment. The core of our simulations was OpenFOAMR or Open Source Field Operation and Manipulation. OpenFOAMR is an open-source CFD software that contains a toolbox for tailored numerical solvers. The algorithm implemented in OpenFOAMR uses the Finite Volume Method on unstructured meshes (see ref. 19).

OpenFOAMR includes pre-processing and post-processing capabilities such as snappyHexMesh and ParaFoam for meshing and visualization, respectively. We also used other open-source software that provides pre-processing and post-processing tools for CFD such as Salome and ParaView. Salome (version 7.3.0) was mainly used to build the geometry of the different models and ParaView (version 4.1.0) to display some of the images.

The real flow domain is a ventricular catheter along with the lateral ventricle where it is placed in. However, our goal is just to compute the flow rate distribution and shear stress in the neighborhood of the ventricular catheter walls, so the influence that the geometry and volume of the ventricle might have on the results is negligible. In view of this fact, the lateral ventricle was modeled as a cylinder (see ref. 6), to facilitate the task of meshing and thus improving the accuracy and computational efficiency.

The cylinder is 75 mm long and its diameter is 16 mm. The inner diameter and outer diameter of the ventricular catheter are 1.5 and 2.5 mm, respectively, and the part of the ventricular catheter inside the cylinder has a length of 60 mm. The configuration and dimensions of the ventricular catheter holes varied in all models. Their geometric features were adjusted following the design principles established in our previous studies (5, 13–15), particularly in our parametric data (14), to obtain an approximately uniform flow rate distribution.

The presented prototype catheters 3D printed included micromanufacturing processes developed for fabrication of functional and true 3D assemblies. Last-generation 3D laser lithography system, included 3D microprinting and maskless lithography, combining an ultra-precise piezo mode for arbitrary 3D trajectories (FBMS) and the high-speed galvo mode (MBFS) for structuring in a layer-by-layer fashion.

For the benchmark testing, we choose our printed catheters our prototype models. A water vase and Indian ink were used for the injection flow technique. This checking method is based and, to a certain extent, follows the studies of Lin et al. (8), Thomale et al. (16), and ours (5). To disclose specifically the flow within the catheter, we did not add a commercially available shunt valve to the set, injecting the ink directly to the catheter using a regular clinical medical pump.

Results

Vector representations of the flow fields within the first 7 s of a ventricular catheter prototype of five segments with 6 holes per segment resulting from CFD 3D analysis are shown in Fig. 4. It is evident that the initial flow is defined within the first 2 s after catheter insertion. As a representative CFD analysis, we present the complete data of a catheter with a hole on its tip (Fig. 5a, b, c). Fluid velocities can then be converted into flows and distributions of flow per segment. The simulations also demonstrate that the velocity patterns are different in this ventricular catheter. Noteworthy, the bulk flow is quite uniform along the catheter, while the flow on the tip hole is negligible (Fig. 5d, e). All diameters and distances are in millimeters. The evolution of the flow distribution shows that the flow through the ventricular catheter segments reaches stationarity after 0.05 s in this model (Fig. 5f). The stationary flow distribution is depicted in all figures in cm^3/day, where the flow is indicated in each ventricular catheter segment. The inlet flow through each segment of each ventricular catheter, as well as the inlet flow per unit area through each segment and the total sum of inlet segment flows, is shown in Fig. 5d. Three-dimensional images show stationary flow in this particular model. These images reveal regions of localized above-average velocities in most holes with a uniform pattern in this model. Figure 5e shows the time evolution of the velocity peak in the model with a hole on its tip represented. U magnitude is a specific volume value used by CFD software. This variable drops very fast from its initial value to its minimum, and then converges slowly to its stationary value (Fig. 5f). Once again, we point out that the physically relevant data correspond to stationary flow results. Ventricular catheter wall shear stress imaging can be seen in Fig. 5g as well. The shear stress peaks converge to

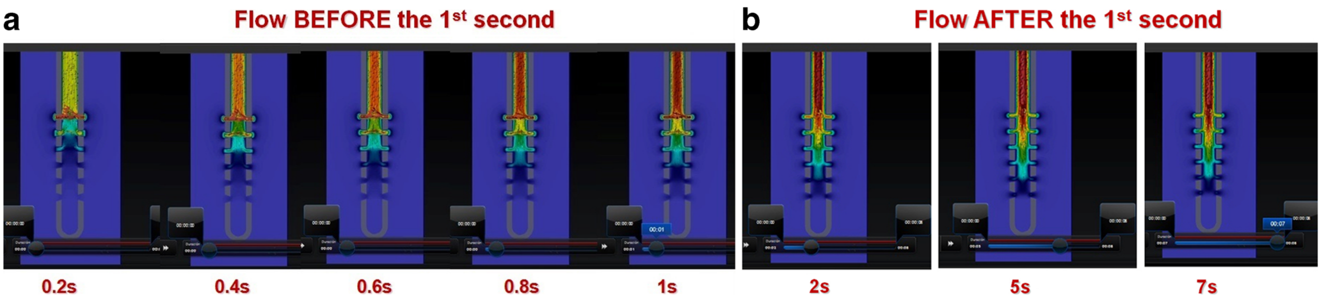

Fig. 4 3D representation of the velocity through the holes and inside a prototype catheter; in here, we disclosed the flow during the first second after primary insertion of the ventricular catheter (**a**), with almost no change in flow until stabilization around the seventh second (**b**). After insertion, clear flow distribution is seen after 2 s

their stationary values in a, basically, decreasing monotonic way for all ventricular catheter models (not shown). The CFD results of a catheter with hole on its tip showed that the flow was not particularly affected with this characteristic.

Several prototypes models were developed. For practical purposes, we present other six new models. Three catheter designs are presented in Fig. 6, while other three catheters depicting their flow are represented in Fig. 7. Using our CFD methodology, we calculated that the flows through the segments distribute evenly in three ventricular catheter prototypes (Fig. 6). Models have a constant flow over the segments. The anteroposterior and left-right components of the velocity vectors, depicted in three dimensions, show the same pattern in prototype models (not shown). These relations are depicted as blue bars along with their segment area (Fig. 7). Catheters represented in Fig. 7 are a variant of catheter showed in Fig. 6a. The scale below each model makes evident that the flow vectors are equally concentrated in all holes and the fluid velocities are there similar in each model, disclosing that all holes drains the CSF uniformly.

Printed catheters digital 3D imposed finite resolution that is the size of a single unit. Several advantages of this 3D digital domain included ideal repeatability, high dimensional accuracy, and the intrinsic capability of low-temperature fabrication using a diverse set of materials. We fabricated three consecutive models (Fig. 8) based on Fig. 6a.

Benchmark testing results in our prototype catheter confirmed our CFD results. Video examination after ink injections into the water vase make possible the analysis of the functionality of segment holes in these parametric ventricular catheters. Representative images of ink-stained water draining into the different catheter segments are depicted in Fig. 9. Initial ink flow during the first second was considered representative.

Discussion

Designing ventricular catheters (VC) with better flow distribution and possibly less prone to obstruction might be influential for the treatment of hydrocephalus. After analyzing the parametric concept behind the optimal flow solution for ventricular catheters (14), we present in this study several model solutions along with 3D printed catheters with basic benchmark testing based on parametric developments. Additional complete CFD data of a catheter with hole on its tip is presented.

In current standard ventricular catheters, for a given extraction pressure at the valve, the volumetric flow rate is determined by the total drainage area, i.e., by the number of holes and their cross sections. The obstruction of some of the holes and then of the catheter lumen by choroid plexus, cells, and macromolecules present in the CSF is the most common cause of shunt malfunction in children. This problem has, consecutively, several factors, including a wrong placement of the ventricular catheter in the ventricle. From a trajectory from the occipital horn, the tip of the VC may contact the septum pellucidum, and the proximal part of the VC may contact the choroid plexus of the atrium part of the ventricle. After evaluating these situations, we deduce that there are, in most cases, *three* different parts of anatomical importance for the VC within the ventricle (Fig. 1): the most distal part; the medium part; and the most proximal part, that is, the one closer to the outlet part of the shunt system. These three different parts of the VC may influence, specifically, in the CSF flow within the catheter. Several authors have considered catheter positioning in previous studies (16, 20). Evidently, in the present work, we consider only obstruction factors related to the CSF flow characteristics in ventricular catheters based on methods of computational fluid dynamics.

The precise mechanism of ventricular catheter occlusion is not known but certainly includes the valve designs (5, 9–11); however, ventricular catheter obstruction may occur with any valve design, so flow factors of the catheter itself are of key importance (5, 12, 14, 16). In standard ventricular catheters, we demonstrated that between more than half of the CSF volume flows through proximal holes (6); evidently, this fact increases the shear stress at the proximal segment. A first step towards the numerical study of the CSF flow in ventricular catheters was done by Lin et al. in (8) using CFD in two dimensions. This work was generalized to

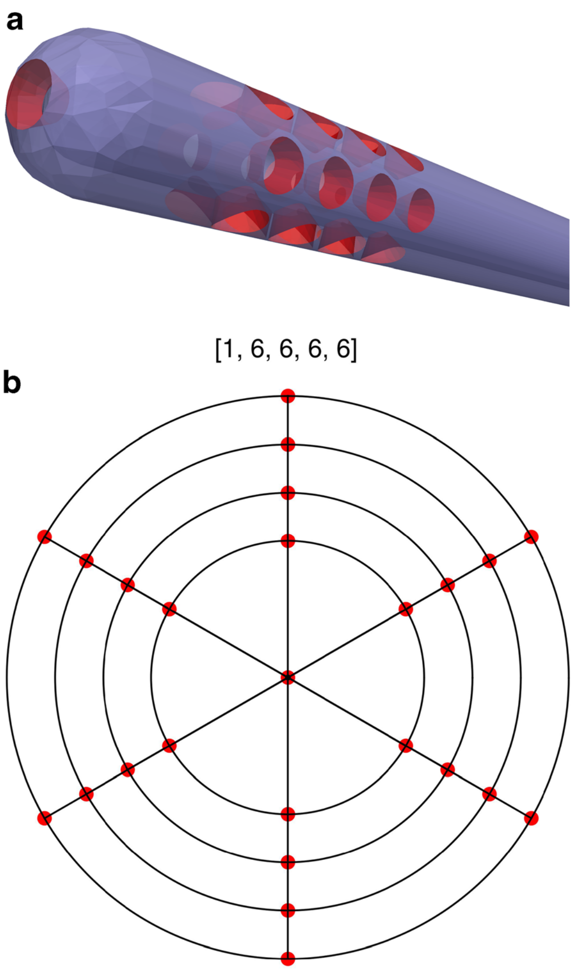

c

Number of holes / Number of segments	24 / 5
Number of holes per segment	[1, 6, 6, 6, 6]
Distance from each segment to the tip	[0.0, 4.25, 5.75, 7.25, 8.75]
Outside radius of the holes in the same segment	[0.5, 0.5, 0.5, 0.5]
Inside radius of the holes in the same segment	[0.3, 0.35, 0.3, 0.25, 0.2]
Inside diameter of the catheter (I.D.)	1.5
Outside diameter of the catheter (O.D.)	2.5
Total sum of hole areas per segment	[0.28, 2.31, 1.7, 1.18, 0.75]
Inlet flow through each segment	[1.63, 17.38, 22.71, 28.2, 29.15]
Inlet flow per unit area through each segment	[5.76, 7.53, 13.39, 23.94, 38.66]
Total sum of inlet segment flows	99.07315

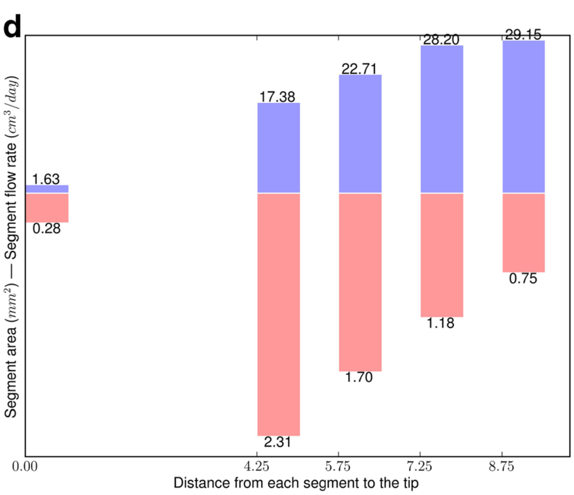

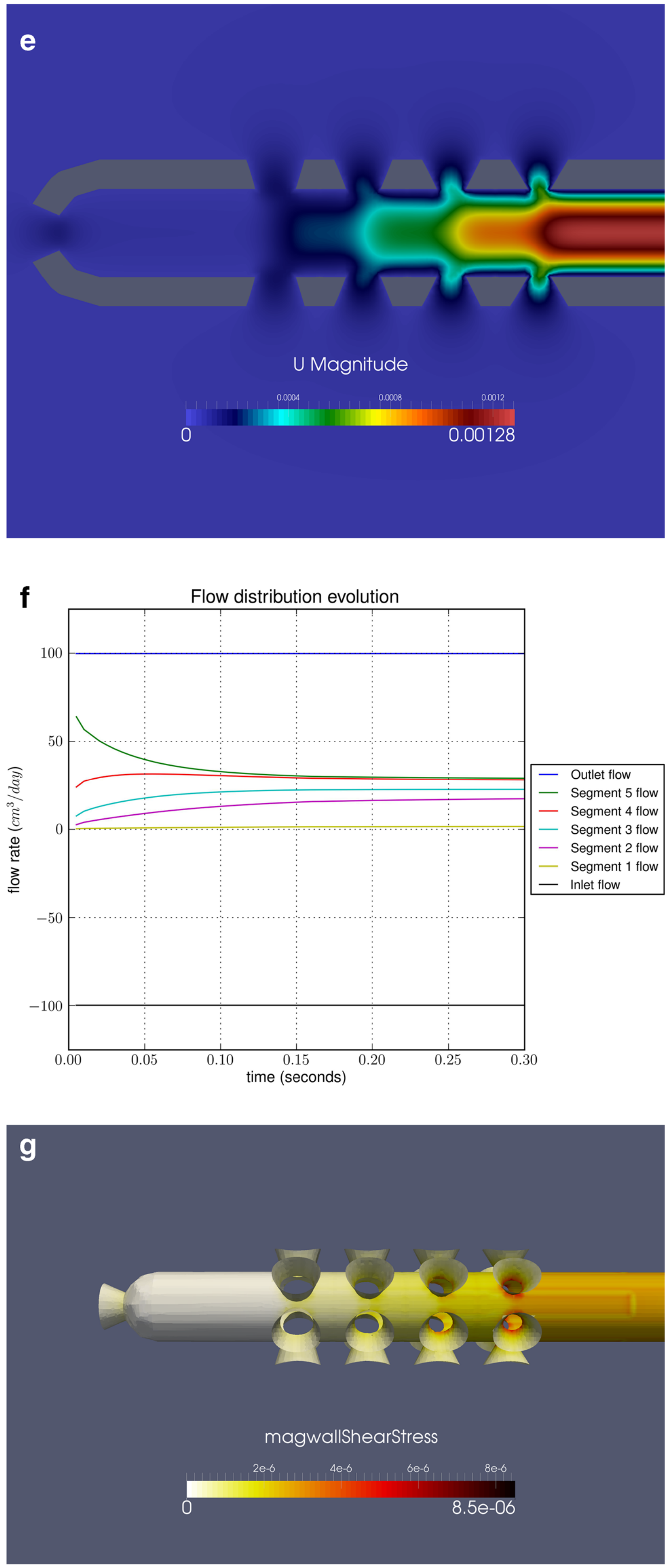

Fig. 5 Imaging representation and numerical specifications of a catheter with a hole on its tip (**a**–**c**). Full analysis and CFD results are shown in **d**–**g**. See text for details. Figure of segment flow rate versus segment area show that the flow on its tip is quite negligible

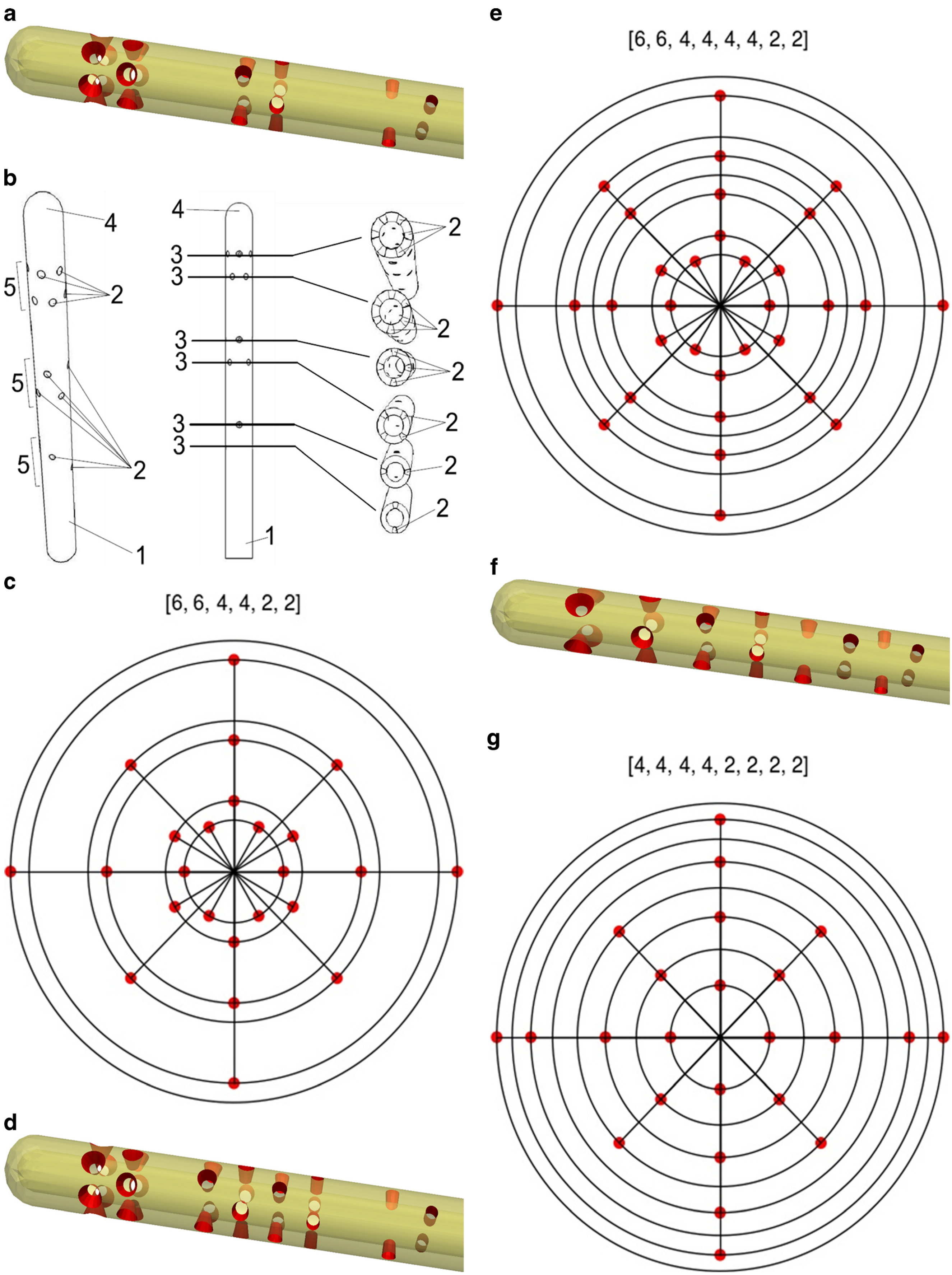
a
b
4
5
2
5
2
5
2
1
4
3
3
3
3
3
3
2
2
2
2
2
2
1
c
[6, 6, 4, 4, 2, 2]
d
e
[6, 6, 4, 4, 4, 4, 2, 2]
f
g
[4, 4, 4, 4, 2, 2, 2, 2]

◀ **Fig. 6** Geometric characteristics of three prototype ventricular catheter models based after parametric development. Models are depicted as 3D images (**a**, **d**, **f**), showing its hole characteristics only in model 1 (**b**) and target design showing segment hole distribution (**c**, **e**, **g**)

three dimensions in (5, 6, 13), where some of the authors of this paper examined how variations of the hole geometry and configuration affect the flow rate distribution per segment and the shear stress at the holes (15). To this end, manifold ventricular catheters were modeled with great geometrical detail and the steady solution of the general Navier-Stokes equation was computed in a domain containing the ventricular catheter under stationary boundary conditions. Based on these results, we formulated a number of basic design principles in (14).

Previously, we evaluated the fluid dynamics of five new ventricular catheter models to estimate flow factors of proximal shunt malfunction (13). These ventricular catheters were of three up to four segments and equidistantly distributed. In our opinion, prototype catheters with a few segments are not efficiently designed, given the short inlet length within the ventricle. Yet, as Thomale et al. (13) reported and coinciding with our results (13), these particular types of catheters have a better flow distribution. On the other hand, catheters with a large number of holes per segment, i.e., more than 8 on its first segment for example, were not physically stable given its

Fig. 8 True 3D catheters included micromanufacturing processes developed for printed solutions based on the catheter presented in Fig. 6d

large initial drainage area; that is, they have a small attachment area to the rest of the catheter. The inherent distal weakness may predispose to break it during insertion, or revision.

Let us underline at this point that the results reported in this paper are only based on three-dimensional flow simulations; hence, they are entirely mathematical, and thus, our results can only be compared with other 3D flow results. We simulated and simplified the ventricle area by modeling it as cylinder. The reason and method details for this can be found in our previous papers (5, 6, 13–15) and in references (18, 19).

Other important contributions regarding the ventricular catheters design came from the Harris and McAllister group (10, 21,

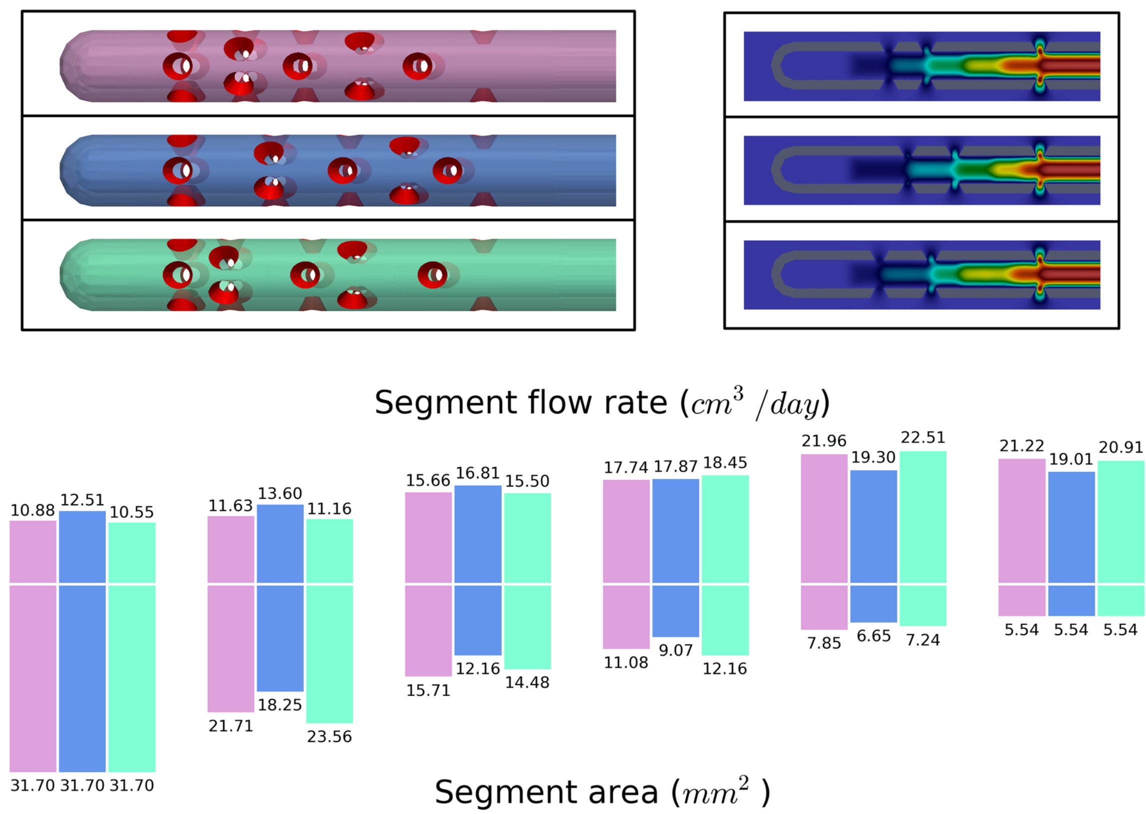

Fig. 7 **a** Depictions of parametric prototype models with CFD results shown on the left. These catheters are based on specifications of catheter showed in Fig. 6a. All catheters have different segment flow rate and segment area, while the flow rate is quite evenly distributed among segments

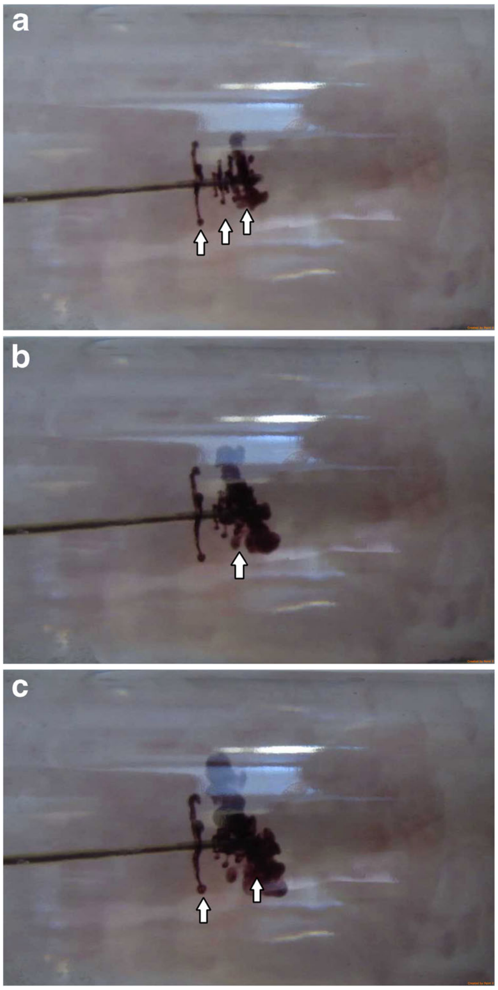

Fig. 9 Initial ink flow during the first second was considered representative during the injection flow technique in this parametric prototype catheter showed in Fig. 7. Images depicting flow during the 0.1 s (**a**) shows three distinct drainage parts of the catheter with most of the flow in the distal part; on 0.6 s (**b**), the medial and distal part of the flow becomes one, while on 0.9 s (**c**), there still independent flow in the distal (most) and proximal part of the catheter

22). Harris and McAllister's previous results on flow through ventricular catheter lumen indicate that a raise in flow, therefore shear stress, increases cell adhesion (22). Their study suggests that cell adhesion generally decreases with increasing hole diameter under flow conditions and stated the need to examine how hole diameter impacts inflammatory-based shunt obstruction (21). Thomale stated that the use of more than two holes, theoretically, did not enhance the amount of drainage through the ventricular catheter (16). This is true, from a hydrodynamic standpoint, only when there is a constant pressure. Certainly, it is a condition not reflected in hydrocephalus. Instead, we entirely agree with Thomale et al. when they affirm that a reason to include more perforations in catheters than actually needed might be the high probability of placing some holes intraventricularly by freehand puncturing. Thus, the amount of perforation holes is simply related to the narrow precision of how ventricular catheters are routinely implanted (13). For this reason, we sought catheters with the adequate number of segments and holes, specifically the precise number of holes per segment.

Several caveats should be emphasized in our study. While our theoretical studies described basic design principles which may help to develop new ventricular catheters with better flow circulation, the whole aim is reducing the possibility of ventricular catheter occlusion. Evidently, this hypothesis requires experimental testing with actual prototype catheters currently under development (23).

On the other hand, the methodology used in all our studies was a powerful mathematical simulation system. Hence, the possibility to have introduced some bias in the samples is reduced to near zero. Therefore, we can generalize the flow results to every ventricular catheter used for the treatment of hydrocephalus. A comprehensive dissertation about the subject is currently available from the University of Tennessee (24). Evidently, the next generation of ventricular catheter presenting an optimized flow still need to be tested on real life situations.

According to the existing literature on the CSF dynamics (2, 4, 25), the CSF has a steady pulsatile behavior where both CSF pressure and volume act in a pulsatile fashion onto the ventricular catheter; see (1, 2, 26) for specific information. This raises the question, to which extent the time-dependent character of the CSF flow modifies our previous results, in particular, our ventricular catheter design principles. Recently (27), we reported using the same principle designs, though in a pulsatile ventricular paradigm. Remarkably, the flow within the catheters did not change significantly under pulsatile conditions.

There are two key factors concerning catheter functionality. One is flow characteristics. The other is material construction. Standard catheter is made of silicone elastomer and its resistance to heat, high flexibility, and biocompatibility makes it well suited for in vivo implantation use (10, 21). Yet, silicone elastomer is a rubber material and this condition certainly has implication in the attraction or adhesion of the cells and forms elements to the ventricular catheter.

If we may say that the optimal ventricular catheter should comprehend a triad of optimum flow, optimum anti-adherent material construction and biocompatibility; once resolved the flow factors in ventricular catheters, we need to name the hitherto anonymous material with anti-adherent characteristics. But, that is another chapter yet to be written.

Compliance with ethical standards

Confict of interest Some of the prototypes modeled in this paper has been used for designing ventricular catheters granted a Spanish patent for MG, AG, JMA (23). CE patent is pending. Specifications for certain catheter prototypes cannot be given for patenting purposes still in process. Some of the models presented are currently in development for commercialization.

References

1. Brinker T, Stopa E, Morrison J, Klinge P (2014) A new look at cerebrospinal fluid circulation. Fluids barriers CNS 11:10
2. Greitz D, Wirestam R, Franck A, Nordell B, Thomsen C, Ståhlberg F (1992) Pulsatile brain movement and associated hydrodynamics studied by magnetic resonance phase imaging. The Monro-Kellie doctrine revisited. Neuroradiology 34:370–380
3. Milhorat TH (1975) The third circulation revisited. J Neurosurg 42: 628–645
4. Penn RD, Basati S, Sweetman B, Guo X, Linninger A (2011) Ventricle wall movements and cerebrospinal fluid flow in hydrocephalus. J Neurosurg 115:159–164
5. Galarza M, Giménez Á, Valero J, Pellicer O, Martínez-Lage JF, Amigó JM (2015) Basic cerebrospinal fluid flow patterns in ventricular ventricular catheters prototypes. Childs Nerv Syst 31:873–884
6. Galarza M, Giménez Á, Valero J, Pellicer O, Amigó JM (2014) Computational fluid dynamics of ventricular ventricular catheters used for the treatment of hydrocephalus: a 3D analysis. Childs Nerv Syst 30:105–116
7. United States Patent Serial No.78887628 (2006) Medtronic Inc. Ventricular catheter Rivulet
8. Lin J, Morris M, Olivero W, Boop F, Sanford RA (2003) Computational and experimental study of proximal flow in ventricular ventricular catheters: technical note. J Neurosurg 99:426–431
9. Bergsneider M, Egnor MR, Johnston M, Kranz D, Madsen JR, McAllister JP 2nd, Stewart C, Walker ML, Williams MA (2006) What we don't (but should) know about hydrocephalus. J Neurosurg 104:157–159
10. Harris CA, McAllister JP (2012) What we should know about the cellular and tissue response causing ventricular catheter obstruction in the treatment of hydrocephalus. Neurosurgery 70:1589–1601
11. Drake J, Kestle JR, Milner R, Cinalli G, Boop F, Piatt J Jr, Haines S, Schiff SJ, Cochrane DD, Steinbok P, MacNeil N (1998) Randomized trial of cerebrospinal fluid shunt valve design in pediatric hydrocephalus. Neurosurgery 43:294–305
12. Cheatle JT, Bowder AN, Agrawal SK, Sather MD, Hellbusch LC (2012) Flow characteristics of cerebrospinal fluid shunt tubing. J Neurosurg Pediatr 9:191–197
13. Galarza M, Giménez Á, Valero J, Pellicer O, Amigó JM (2015) New designs of ventricular ventricular catheters for hydrocephalus by 3-D computational fluid dynamics. Childs Nerv Syst 31:37–48
14. Galarza M, Giménez A, Pellicer O, Valero J, Amigó JM (2016) Parametric study of ventricular ventricular catheters for hydrocephalus. Acta Neurochir (Wien) 158:109–115 discussion 115–116
15. Giménez Á, Galarza M, Pellicer O, Valero J, Amigó JM (2016) Influence of the hole geometry on the flow distribution in ventricular ventricular catheters for hydrocephalus. Biomed Eng 15:5–19
16. Thomale UW, Hosch H, Koch A, Schulz M, Stoltenburg G, Haberl EJ, Sprung C (2010) Perforation holes in ventricular ventricular catheters—is less more? Childs Nerv Syst 26:781–789
17. Weisenberg SH, TerMaath SC, Seaver CE, Killeffer JA (2016) Ventricular catheter development: past, present, and future. J Neurosurg 125:1504–1512
18. Tenti G, Sivaloganathan S, Drake JM (2008) Mathematical modeling of the brain: principles and challenges. Neurosurgery 62:1146–1157
19. Versteeg H, Malalasekra W (2007) An introduction to computational fluid dynamics: the finite volume method, 2nd edn, rev. Prentice Hall, Harlow, England; New York
20. Kehler U, Klöhn A, Heese O, Gliemroth J (2003) Hydrocephalus therapy: reduction of shunt occlusions using a peel-away sheath. Clin Neurol Neurosurg 105:253–255
21. Harris CA, McAllister JP II (2011) Does drainage hole size influence adhesion on ventricular ventricular catheters? Childs Nerv Syst 27:1221–1232
22. Harris CA, Resau JH, Hudson EA, West RA, Moon C, McAllister JP II (2010) Mechanical contributions to astrocyte adhesion using a novel in vitro model of ventricular catheter obstruction. Exp Neurol 222:204–210
23. Spanish Patent Serial No.201400178 (2015). Ventricular catheter with improved flow for hydrocephalus treatment
24. Weisenberg, SH, "Improving ventricular catheter design through computational fluid dynamics" Master's Thesis, University of Tennessee, 2016. http://trace.tennessee.edu/utk_gradthes/3817
25. Linninger AA, Tsakiris C, Zhu DC, Xenos M, Roycewicz P, Danziger Z, Penn R (2005) Pulsatile cerebrospinal fluid dynamics in the human brain. IEEE Trans Biomed Eng 52:557–565
26. Wagshul ME, Chen JJ, Egnor MR, McCormack EJ, Roche PE (2006) Amplitude and phase of cerebrospinal fluid pulsations: experimental studies and review of the literature. J Neurosurg 104: 810–819
27. Giménez Á, Galarza M, Thomale U, Schuhmann MU, Valero J, Amigó JM (2017) Pulsatile flow in ventricular catheters for hydrocephalus. Philos Trans A Math Phys Eng Sci 375(2096). doi:10.1098/rsta.2016.0294